Immobilizing molecular Ru complexes on a protective ultrathin oxide layer of p-Si electrodes towards photoelectrochemical CO_2 reduction

Maxime Laurans, Jordann A. L. Wells and Sascha Ott

Department of Chemistry – Ångström Laboratory, Uppsala University, Box 523, 75120 Uppsala, Sweden. E-mail: sascha.ott@kemi.uu.se

Table of contents:

NMR spectroscopy of complex (1)

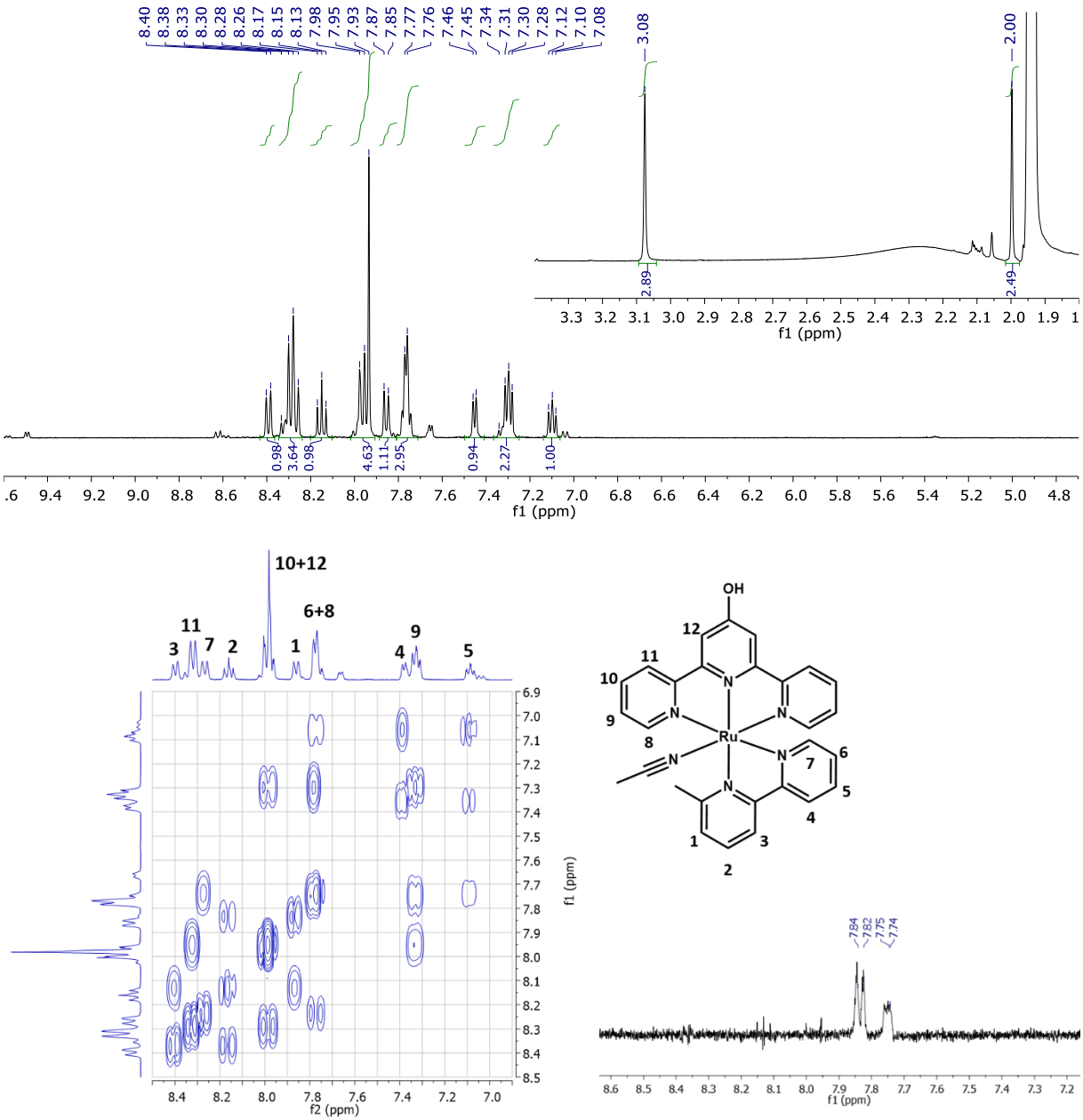

Figure S1. 1D ^{1}H (top) and 2D COSY (left) and 1D difference NOE (with a pulse set at δ=3.04 ppm, s, 3H, -CH_3) (right) NMR spectra of **(1)** in CD_3CN/400 MHz.

X-ray Crystallography

Specific for **(2)**: The methylbipyridine ligand exhibits a positional disorder where the Me group is either *cis* or *trans* to the coordinated chloride ligand (occupancies: *trans* = 80 %, *cis* = 20 %). The protons for one lattice H_2O molecule were located on the difference map, and the O-H and H-H distances were fixed to 0.95 Å and 1.50 Å, respectively. Another lattice water molecule is disordered over two sites (75 % and 25 % occupancies), and the protons could not be located on the difference map, or led to unstable refinement. The non-coordinated chloride ligand is disordered over two sites (75 % and 25 % occupancies). The Ru1 complex showed further disorder on the bipyridine ligand by analysis of the Fourier difference map. Unfortunately, modelling this disorder did not lead to stable refinement, and the corresponding *trans* MeCN ligand could not be located in the Fourier difference map. The disorder was attempted to be modelled in three parts with occupancies 0.375, .0375, and 0.25 for parts 1, 2, and 3 respectively. Parts 1 and 2 represent the positional *cis/tans* disorder of the methylbipyridine ligand with respect to the MeCN ligand. Part 3 represents the positional disorder of the methylbipyridine and MeCN ligands, and is a mirror plane reflection of Part 1. This is schematically represented in **Figure S2(B)**.

Specific for **(1)**: While the crystals grown were of good quality, low intensity diffraction was obtained even with prolonged exposure times. This may be due to the small size of the crystals, which were very thin needles. We expect that a high intensity X-ray source (e.g. synchrotron) would be required to obtain higher resolution data. The dataset presented here is suitable for the purpose of identifying the complex and broadly discussing the molecular geometry. The methylbipyridine ligands on Ru1 and Ru2 exhibit a positional disorder where the Me group is either *cis* or *trans* to the coordinated acetonitrile (Ru1 occupancies: *trans* = *cis* = 50 %; Ru2 occupancies: *trans* = 75 %, *cis* = 25 %). There is residual electron density near the acetonitrile ligand which corresponds to a tertiary disordered position for the methylbipyridine ligand, however stable refinements could not be obtained after modelling this disorder. One of the non-coordinating PF_6 anions exhibits a positional disordered which was modelled as two parts of equal occupancy. The protons for a lattice H_2O molecule were located on the difference map, and the O-H and H-H distances were fixed to 0.95 Å and 1.50 Å, respectively. The Olex2 solvent mask function was employed to remove disordered lattice solvent molecules which could not be successfully modelled. A 733.1 Å void was removed containing 188.9 electrons, which was ascribed to four diethyl ether molecules and two water molecules (per unit cell).

CCDC 2059979-2059980 contain the supplementary crystallographic data for this paper. The data can be obtained free of charge from The Cambridge Crystallographic Data Centre via www.ccdc.cam.ac.uk/structures.

Table S1. Selected bond lengths (Å) and angles (°) for **(2)**, and **(1)**.

Parameter	(2)	(1)	
		Ru1	Ru2
Ru-N1	2.06 (1)	2.080 (3)	2.073 (3)
Ru-N2	1.94 (1)	1.975 (3)	1.978 (3)
Ru-N3	2.06 (1)	2.068 (3)	2.070 (3)
Ru-N4	2.06 (1)	2.198 (8)	2.056 (4)
		1.997 (7)	2.16 (2)
Ru-N5	2.06 (1)	2.085 (7)	2.116 (7)
		2.029 (8)	2.04 (2)
Ru-X	2.413(4)	2.039 (4)	2.038 (5)
	X = Cl	X = MeCN	

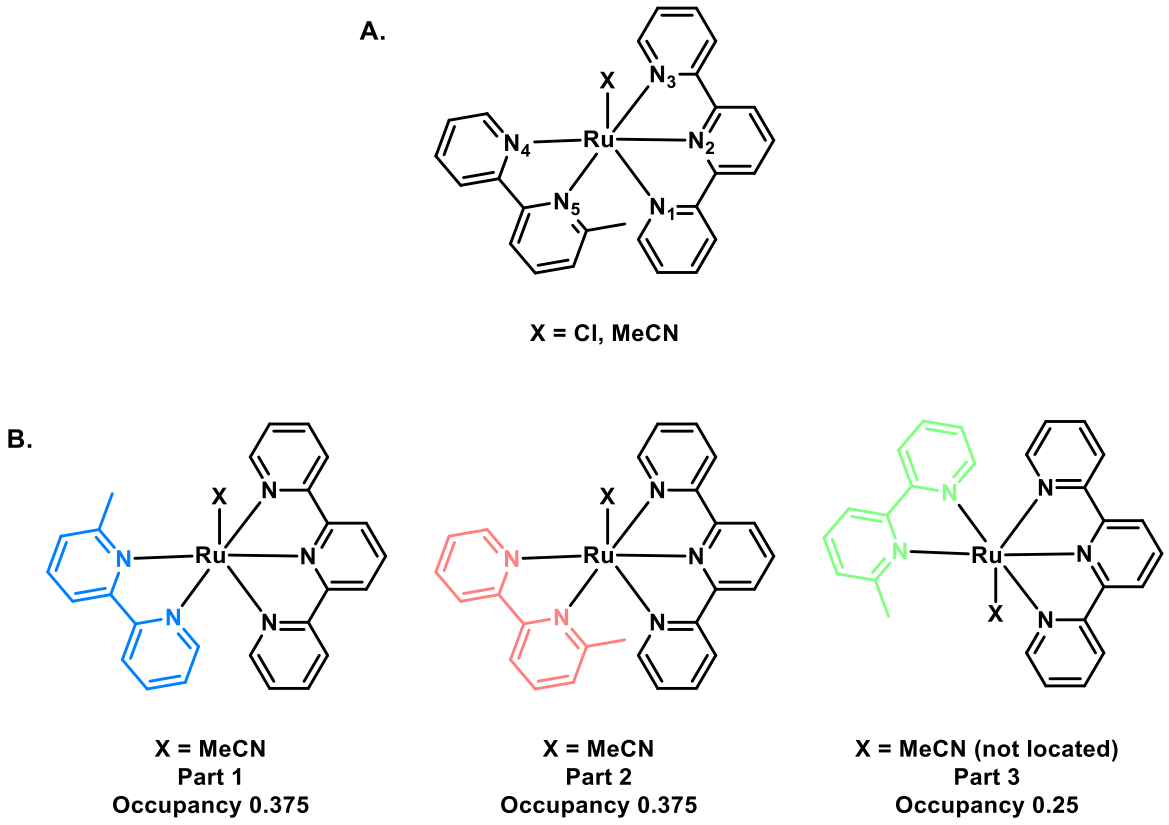

Figure S2. A. Numbering convention for **Table S1**. B. Positional disorder in the crystal structure of **(2)**, which could not be modelled in order to obtain stable refinement.

Table S2. Crystal data and structure refinement.

Compound	**Ru Cl**	**Ru PF6**
Chemical formula	$(C_{26}H_{21}ClN_5ORu)\ H_2O{\cdot}Cl{\cdot}O$	$2(C_{28}H_{24}N_6ORu)\ 4(F_6P){\cdot}H_2O{\cdot}C_4H_{10}O$
M_r	625.46	1795.22
Crystal system, space group	Monoclinic *P21/n*	Triclinic $P\bar{1}$
Temperature (K)	170	170
***a*, *b*, *c* (Å)**	8.770 (6) 25.712 (16) 11.115 (8)	13.989 (3) 14.256 (3) 23.355 (4)
α, β, γ (°)	- 96.765 (14) -	90.689 (6) 96.845 (6) 118.958 (5)
***V* (Å³)**	2489 (3)	4033.3 (2)
Z	4	2
Radiation type	Mo Kα	Mo Kα
μ (mm^{-1})	0.89	0.56
Crystal size (mm)	0.36 × 0.08 × 0.08	0.36 × 0.25 × 0.10
Diffractometer	Bruker D8 APEX-II	Bruker D8 APEX-II
Absorption correction	Multi-scan	Multi-scan
T_{min}, T_{max}	0.422, 0.745	0.694, 0.746
No. of measured, independent and observed [I > 2s(I)] reflections	23121 4402 2465	210324 22061 11762
R_{int}	0.190	0.068
$(\sin\theta/\lambda)_{max}$ ($Å^{-1}$)	0.595	0.690
R*[F^2 > 2σ (F^2)], *wR*(F^2), *S	0.100, 0.268, 1.10	0.061, 0.154, 1.12
No. of parameters	354	1180
No. of restraints	102	1494
H-atom treatment	Independent and constrained	Independent and constrained
$\Delta\rangle_{max}$, $\Delta\rangle_{min}$ (e $Å^{-3}$)	1.38, −1.57	1.21, −0.81
CCDC No.	2059979	2059980

Cyclic Voltammetry in solution

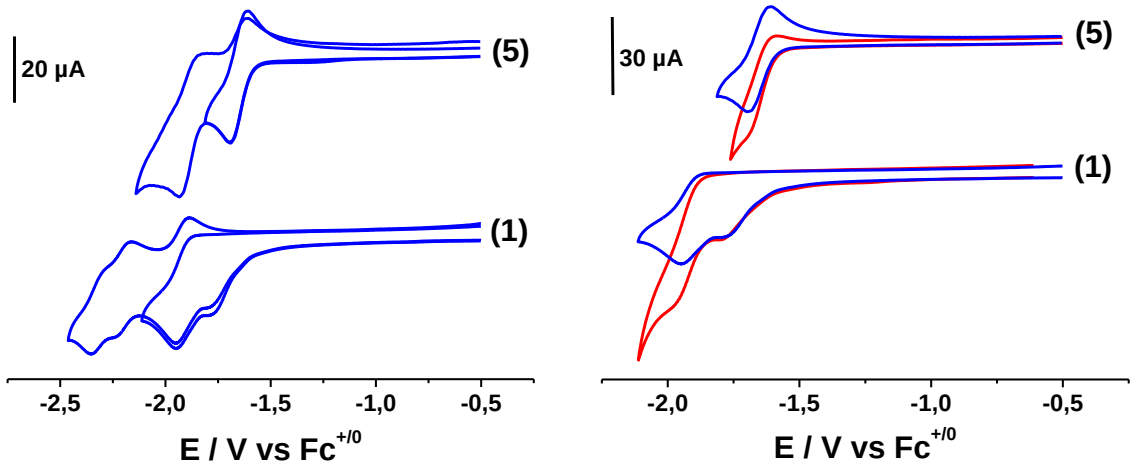

Figure S3. Cyclic voltammograms of **(1)** and **(5)** (1 mM) under Ar (blue) and under CO_2 (red). All experiments were done in 0.1 M $TBAPF_6$ in CH_3CN, *v* = 200 mV/s.

X-ray Photoelectron Spectroscopy

Calibration:

The calibration was made on the survey spectrum and was based on the Si2p peak. Following deconvolution of the signal in two contributions, one for the silicon oxide and one for the bulk silicon, the latest at 99.4 eV.

Deconvolution of the C1s and Ru3d3/2 peak

Ru 3d(3/2) contribution area was imposed to be 0.6667*Ru3d (5/2) contribution area and a spin-orbit splitting of + 4.17 eV.[1] Two C1s contributions were added and fitted according to the expected C atoms environments.

All the fit operations for C1s+Ru3d (3/2), Ru3d (5/2) and N1s peaks gave a satisfying residual STD between 1.02 and 1.64.

Ratios of atomic percentage

The atomic percentage ratios N/Ru were determined from high resolution spectra after deconvolution of the C1s+Ru3d and N1s photopeaks.

Table S3. RSF (relative sensitivity factors) based on Casa XPS v 2.3.22PR1.0 software values.

Element	Ru 3d		N 1s	Si 2p	C1s
	5/2	3/2			
RSF	7.39	5.1	1.8	0.817	1

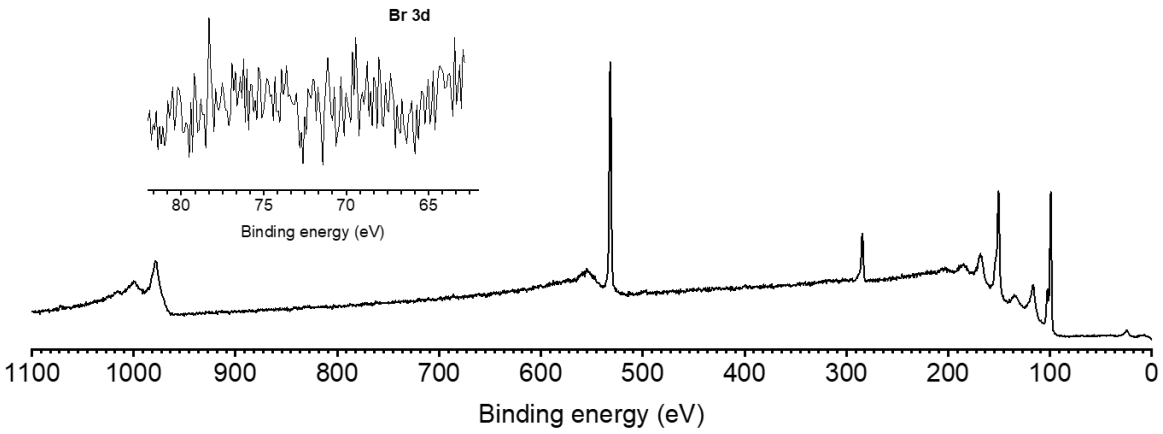

Figure S4. XP survey spectrum of 3-bromopropyltrimethoxysilane on native silicon oxide, (inset: high resolution spectrum of Br3d region).

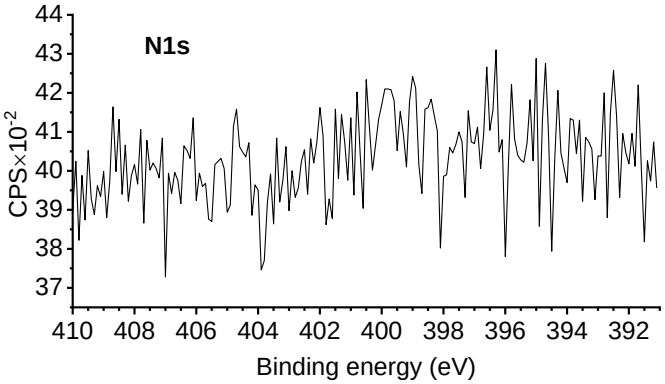

Figure S5. High resolution XPS N1s region of p-Si/SiO_2/Br after 4 days at room temperature in a 2.5mM DIPEA solution in CH_3CN.

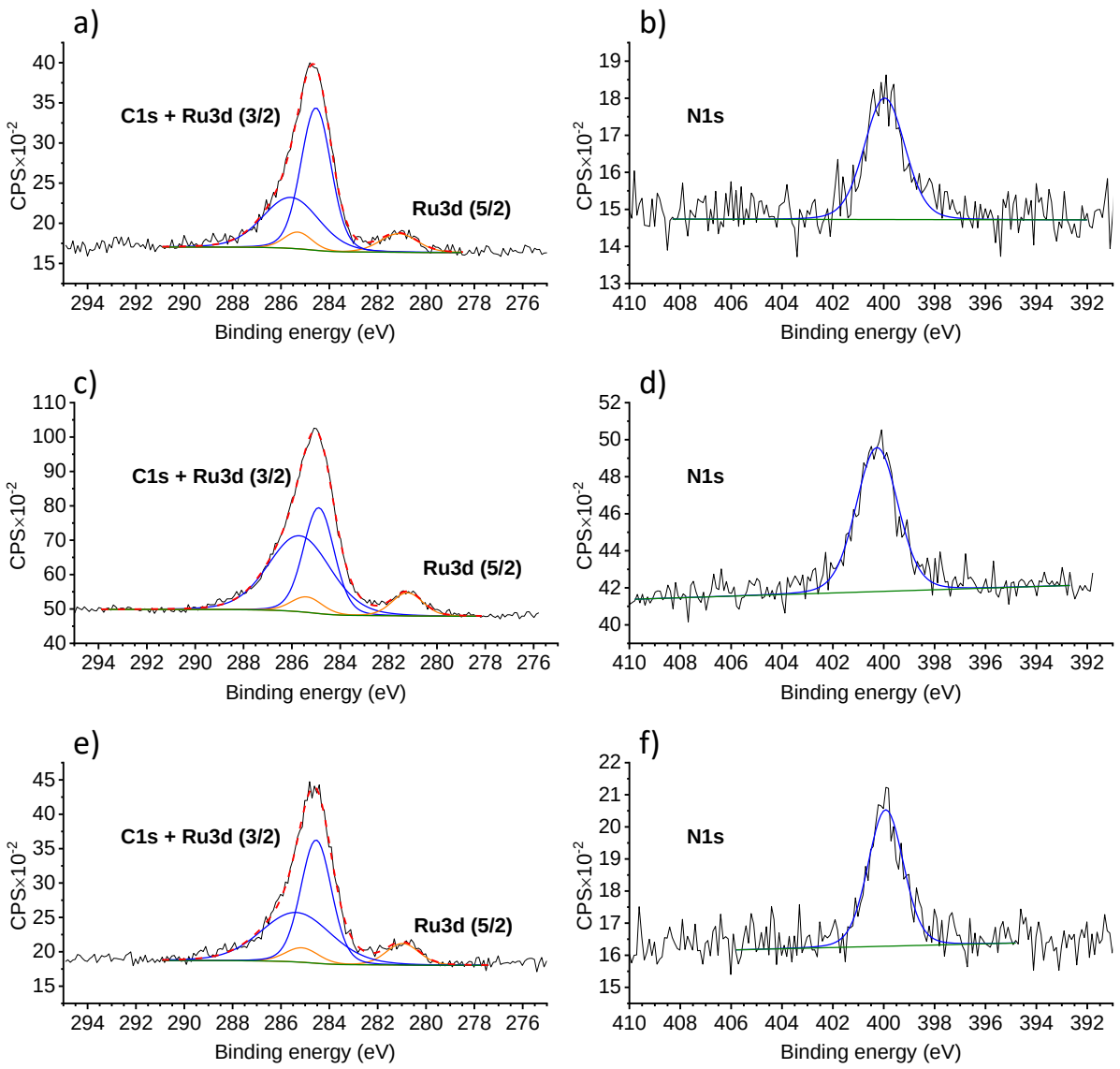

Figure S6. High resolution XPS C1s/Ru3d and N1s regions of p-Si/SiO_2/[Ru] after 5min. sonication in CH_3CN (a and b) and after 5min. sonication in $TBAPF_6$ 0.1M in CH_3CN (c and d) and after 20min. in $TBAPF_6$ 1M in CH_3CN (e and f).

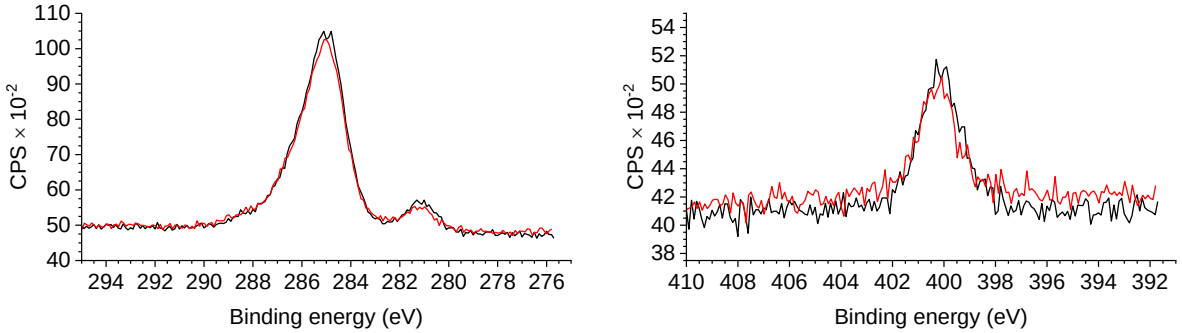

Figure S7. High resolution XPS C1s/Ru3d (left) and N1s (right) regions of p-Si/SiO_2/[Ru] before (black) and after (red) 5min. sonication in $TBAPF_6$ 0.1M in CH_3CN.

Photoelectrochemistry study

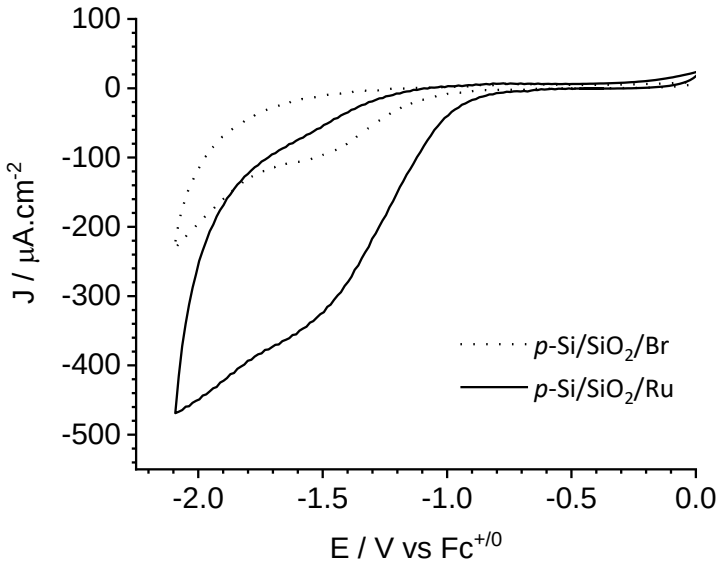

Figure S8. Cyclic voltammograms of p-Si/SiO_2/Br after 4 days in 2.5 mM DIPEA in acetonitrile and p-Si/SiO_2/[Ru] under one sun illumination ($TBAPF_6$ 1M in CH_3CN, v=1V.s^{-1}).

Table S4. Reported photovoltages obtained for catalysts for reductive transformations at illuminated p-Si.

Assembly	Related Molecular specie or Catalyst	Measured Photovoltage at illuminated p-Si	Dark electrode	Ref.
Immobilized				
Si/SiO_2/[Ru]	Complex **(1)**	+570 mV	n^+-Si	This work
p-Si | BisPNP-Ni	H^+ from [H(dmf)]OTf	+210 mV	n^+-Si|BisPNP-Ni	(2)
Zr(NDI)|TiO2@Si	NDI reduction	+330 mV	Zr(NDI)|TiO2@FTO	(3)
In solution				
[Fe_2(µ-bdt)$(CO)_6$]	[Fe_2(µ-bdt)$(CO)_6$]	+500mV	Glassy Carbon	(4)
Re(bipy-But)$(CO)_3$Cl	Re(bipy-But)$(CO)_3$Cl	+500 mV	Pt	(5)

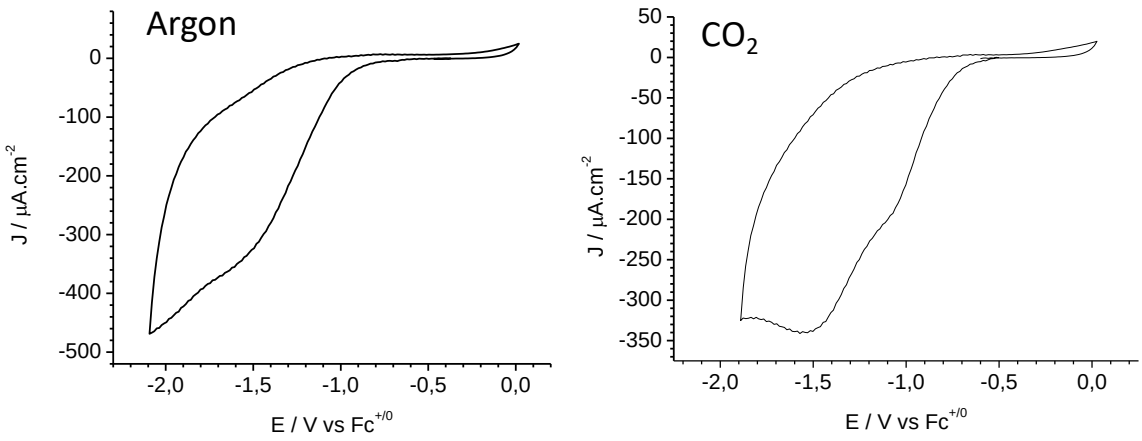

Figure S9. Cyclic voltammograms of p-Si/SiO_2/[Ru] photoelectrodes under one sun illumination ($TBAPF_6$ 1M in CH_3CN, v = 1V.s^{-1}) under Ar (left) and CO_2 (right) saturated conditions.

Discussion

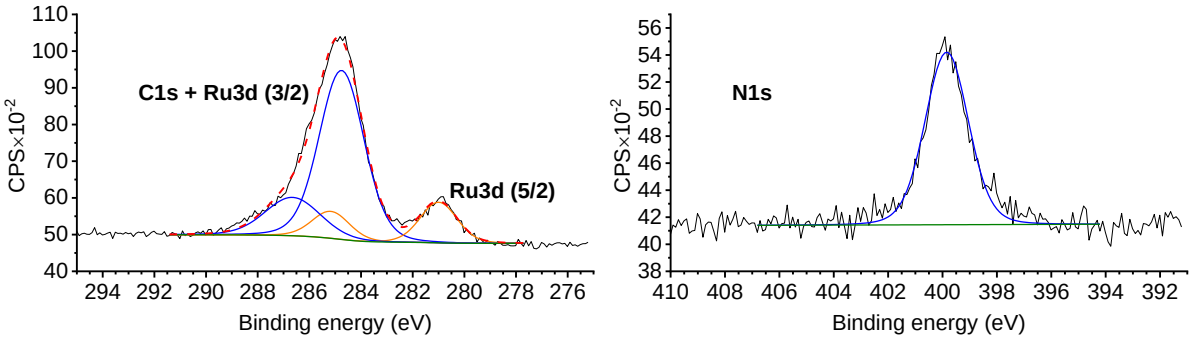

Figure S10. High resolution XPS C1s/Ru3d and N1s regions of p-Si/SiO_2/[Ru] on 3-propyltrimethoxysilane layer after 5 min sonication in $TBAPF_6$ 0.1M in CH_3CN.

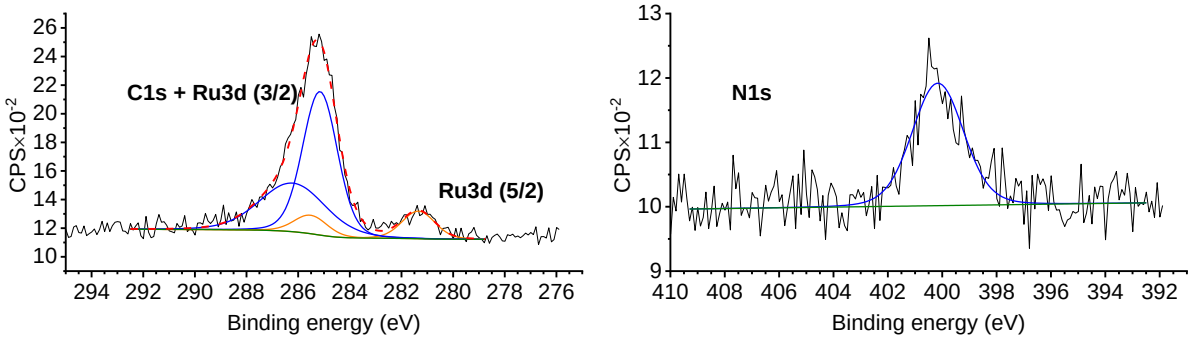

Figure S11. High resolution XPS C1s/Ru3d and N1s regions of p-Si/SiO_2/[Ru] without siloxane layer after 5 min sonication in $TBAPF_6$ 0.1M in CH_3CN.

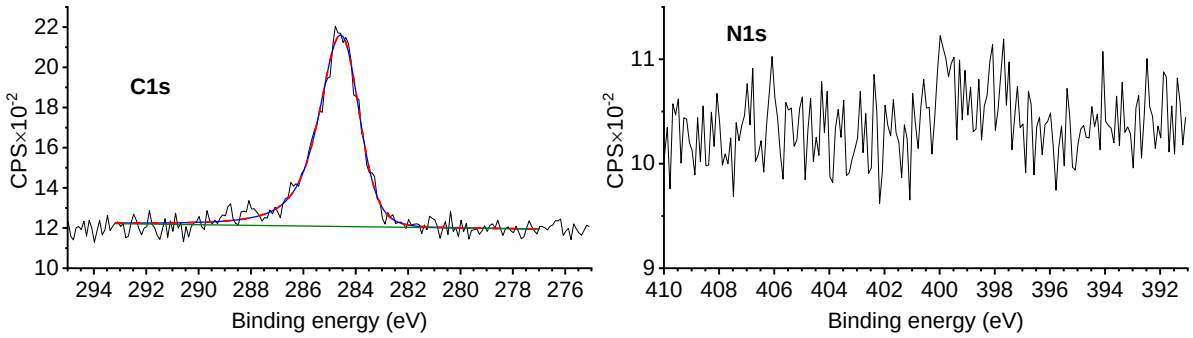

Figure S12. High resolution XPS C1s/Ru3d and N1s regions of p-Si/SiO_2/**(5)** after 5 min sonication in $TBAPF_6$ 0.1M in CH_3CN.

References

(1) Morgan, D. J. *Surface and Interface Analysis* **2015**, *47* (11), 1072–1079.
(2) J. M. Gurrentz and M. J. Rose, *J. Am. Chem. Soc.*, 2020, **142**, 5657–5667.
(3) A. M. Beiler, B. D. McCarthy, B. A. Johnson and S. Ott, *Nat. Commun.*, 2020, **11**, 5819.
(4) B. Kumar, M. Beyler, C. P. Kubiak and S. Ott, *Chem. – Eur. J.*, 2012, **18**, 1295–1298.
(5) B. Kumar, J. M. Smieja and C. P. Kubiak, *J. Phys. Chem. C*, 2010, **114**, 14220–14223.